J. Biochem. 2009;146(4)581–590
doi:10.1093/jb/mvp107

Photocontrol of Calmodulin Interaction with Target Peptides using Azobenzene Derivative

Hideki Shishido, Masafumi D. Yamada, Kazunori Kondo and Shinsaku Maruta*

Division of Bioinformatics, Graduate School of Engineering, Soka University, Hachioji, Tokyo 192-8577, Japan

Received March 31, 2009; accepted June 22, 2009; published online July 15, 2009

Calmodulin (CaM), a physiologically important Ca^{2+}-binding protein, participates in numerous cellular regulatory processes. It is dumbbell shaped and contains two globular domains connected by a short α-helix. Each of the globular domains has two Ca^{2+}-binding sites, the EF hands. CaM undergoes a conformational change upon binding to Ca^{2+}, which enables it to bind to specific proteins for specific responses. Here, we successfully photocontrolled CaM binding to its target peptide using the photochromic compound *N*-(4-phenylazophenyl) maleimide (PAM), which reversibly undergoes *cis–trans* isomerization upon ultraviolet (UV) and visible (VIS) light irradiation. In order to specifically incorporate PAM, CaM mutants having reactive cysteine residues in the functional region were prepared; PAM was stoichiometrically incorporated into the cysteine residues in these mutants. Further, we prepared the target peptide, M13, fused with yellow fluorescent protein (YFP) to monitor the CaM–M13 peptide interaction. The binding of the PAM–CaM mutants, N60C, D64C and M124C, to M13–YFP was reversibly photocontrolled upon UV–VIS light irradiation at appropriate Ca^{2+} concentrations.

Key words: azobenzene, calmodulin, nanomachine, photochromic molecule, photo-regulation.

Abbreviations: ABDM, 4,4′-azobenzene-dimaleimide; CaM, calmodulin; Ca^{2+}/CaM, CaM in a Ca^{2+}-dependent manner; DMF, *N*,*N*′-dimethylformamide; NMR, nuclear magnetic resonance; PAM, *N*-(4-phenylazophenyl) maleimide; PCR, polymerase chain reaction; RLCs, regulatory light chains; SEC–HPLC, size-exclusion chromatography combined with high-performance liquid chromatography; smMLCK, smooth muscle myosin light chain kinase; skMLCK, skeletal muscle myosin light chain kinase; S1, subfragment-1; UV, ultraviolet; VIS, visible; YFP, yellow fluorescent protein; WT, wild-type.

In virtually every eukaryotic cell, calmodulin (CaM) plays a significant role in signalling and regulatory events in many calcium-dependent processes. The structure of CaM has been particularly conserved throughout the evolution of eukaryotes. Many of the target proteins of CaM are enzymes whose activity is stimulated by association with CaM in a Ca^{2+}-dependent manner (Ca^{2+}/CaM) (*1*, *2*); for example, Ca^{2+}/CaM binds to and activates smooth muscle myosin light chain kinase (smMLCK) that plays a critical role in the regulation of smooth muscle contraction (*3*). CaM is a relatively small protein consisting of 148 amino acid residues and has two globular domains that are connected by a long central helix. Both domains of CaM contain two pairs of Ca^{2+} binding sites, the so-called EF hand motifs (*4*, *5*). The EF hand is a helix–loop–helix structural domain and its six Ca^{2+} ligands bind to Ca^{2+} (*6*). There are four EF hands in CAM, which each bind to four Ca^{2+}. Binding of Ca^{2+} to the EF hand of CaM results in conformational changes within each EF hand; this assumed conformation is considerably less open than the previous one, with exposed hydrophobic clefts that are available for target binding (*7*). CaM target proteins have relatively short CaM-binding peptides, which include the M13 peptide and IQ motif. The M13 peptide, which consists of 20 residues and is a part of skeletal muscle myosin light chain kinase (skMLCK), has been shown to form a 1 : 1 complex with Ca^{2+}/CaM (*8*, *9*).

Light irradiation brings about reversible configurational changes in photochromic compounds. Therefore, it is applied to dimmer materials, optical storage materials, indicator materials, etc. (*10–12*). In recent years, the application of photochromic compounds to functional biomolecules has been receiving considerable attention. The potential applications of these biomolecules include their use in biosensors, photocontrol of industrial enzymes, medical treatment, and the study of cell functions. On irradiation with ultraviolet (UV) and visible (VIS) light, azobenzene, a well-studied photochromic compound, reversibly isomerizes between its *cis* and *trans* forms (*13*, *14*). The *cis–trans* isomerization of an azobenzene derivative cross-linked to a synthetic α-helical peptide induced by UV/VIS photo-irradiation has been demonstrated to induce a reversible change in the secondary structure of the peptide, *i.e.* from a helical to a random coil structure, and vice versa (*15*, *16*). Further, the incorporation of photochromic groups into enzymes, such as papain and glucose oxidase, photo-modulates their activity (*17*, *18*).

*To whom correspondence should be addressed. Tel: +81-426-91-9443, Fax: +81-426-91-9312, E-mail: maruta@soka.ac.jp

We have previously demonstrated the possible application of an azobenzene derivative 4,4′-azobenzenedimaleimide (ABDM) in regulating a conformational change in skeletal muscle myosin and kinesin. The azobenzene derivative was incorporated into the SH1–SH2 region of skeletal muscle myosin subfragment-1 (S1), which is a potential energy-transducing site. We had investigated the global conformational change in S1 that was induced by the *cis–trans* isomerization of the cross-linked ABDM in response to UV/VIS light irradiation. It was demonstrated that the *cis–trans* isomerization of ABDM promotes a swing in the lever arm of S1 in a direction opposite to that of the swing induced by ATP binding (*19*). *N*-(4-phenylazophenyl) maleimide (PAM), another azobenzene derivative, was incorporated into the single reactive cysteine residue in loops L11 and L12 of the kinesin mutants. Kinesin is an ATP-driven motor protein. Kinesin modified with PAM exhibited a reversible alteration in the ATPase activity accompanied with *cis–trans* isomerization upon UV/VIS light irradiation (*20*).

In this study, we demonstrated reversible photocontrol of CaM binding to a target peptide by UV–VIS light irradiation using the photochromic compound, PAM. Because CaM regulates numerous functional proteins and cellular regulatory processes, photocontrol of CaM function will enable the regulation of numerous functional proteins and cellular regulatory processes. It will have a wide application in the study of cellular regulation.

EXPRIMENTAL PROCEDURES

Expression and Purification of Proteins—The pET3a vector (Novagen, Madison, WI, USA) encoding mouse wild-type (WT) CaM plasmid was used as the template for the PCR reactions, and fragments for cloning mutant CaM plasmids in the pET3a vector were generated. Site-directed mutagenesis of CaM was performed by self-ligation with primers using *Escherichia coli* DH5α. These plasmids were transformed into *E. coli* BL21 (DE3) pLysS for expression. CaMs were purified to homogeneity by one-step phenyl Sepharose CL-4B (GE Healthcare, Piscataway, NJ, USA) column chromatography, as previously described by Persechini *et al*. (*21*). SDS–PAGE was performed and the purity of the fragments was confirmed by Coomassie staining of the gel. The purified CaMs were dialysed against 30 mM NaCl, 30 mM Tris–HCl (pH 7.5) and 1 mM DTT and were stored at −80°C until further use.

Engineered M13-yellow fluorescent protein (YFP) cDNA was constructed by inserting the M13 peptide sequence (RWKKNFIAVSAANRFKKISS) followed by the EYFP sequence as follows. PCR was used to generate the M13 peptide sequence encoded in the pEYFP-C1 by self-ligation with a vector (Clontech, Palo Alto, CA, USA) and primers using *E. coli* DH5α. This plasmid was the template for PCR to generate the fragment to be used for subcloning cDNA of the M13 peptide-linked EYFP in the pET21a expression vector (Novagen, Madison, WI, USA). This plasmid was transformed into *E. coli* BL21 (DE3) for expression. M13-YFP was purified using a Ni-chelating column that had been equilibrated with a native buffer (300 mM NaCl, 100 mM Tris–HCl (pH 7.5) and 0.2 mM β-ME). The column was washed consecutively with native buffer containing 10 mM imidazole and then with a buffer containing 25 mM imidazole. M13-YFP was eluted with 100 mM imidazole in native buffer, and the purity was confirmed by SDS–PAGE. The purified M13-YFP was dialysed against 100 mM NaCl, 30 mM Tris–HCl (pH 7.5) and 1 mM DTT, and was stored at −80°C until use. The characteristics of the CaM mutants thus prepared were confirmed by phosphorylation of the regulatory light chain of smooth muscle myosin by smMLCK with CaM (*22*) as determined by urea–glycerol PAGE.

Modification of the Mutated Site in CaM using PAM—The CaMs were desalted on a Sephadex™ G-50 Fine (GE Healthcare) column. For the modification of the mutated site in CaM, 50 mM CaM and 100 mM PAM were made to react in 30 mM NaCl, 30 mM imidazole-HCl (pH 7) and 2% *N*,*N*′-dimethylformamide (DMF) for 60 min at 25°C. The PAM-mediated modification reactions were terminated by the addition of 5 mM DTT. Modified CaM was isolated from the unreacted reagents using a Sephadex™ G-50 Fine column. Stoichiometry of the incorporated PAM against that of CaM was performed based on the absorption spectra obtained using an extinction coefficient of 13,380/M/cm at 350 nm for PAM in 30 mM NaCl, 30 mM imidazole-HCl (pH 7) and 2% DMF.

Photo-irradiation for Isomerization of PAM and PAM–CaM—The isomerization of PAM and PAM–CaMs was performed at 0°C using UV light irradiation generated by a Black-Ray lamp (16 W; UVP, Upland, CA, USA) at 366 nm for induction of the *cis* state and by VIS light irradiation using a room fluorescent lamp (27 W) for induction of the *trans* state.

Size-exclusion Chromatography Coupled with High-performance Liquid Chromatography—Size-exclusion chromatography coupled with high-performance liquid chromatography (SEC–HPLC) was performed on a TSKgel G3000SW column (TOSOH, Tokyo, Japan; particle size: 10 mm, internal diameter: 7.5 mm, length: 30 cm, injection volume: 20 μl) with a fraction range of 10–500 kDa. The samples were eluted with Ca-EGTA buffers, prepared as described by Tsien and Pozzan (*23*), containing 100 mM NaCl and 30 mM imidazole-HCl (pH 7.0) at a flow rate of 1 ml/min with monitoring of the absorbance at 230 nm and with an excitation wavelength of 475 nm and monitoring of fluorescence at 527 nm.

RESULTS

Preparation of CaM Mutants Having a Cysteine Residue in the Functional Region—The characteristic structure of the EF hand of CaM or the hydrophobic residue of CaM abundant in amino acid sequences is important for binding to Ca^{2+} or for interaction with a CaM target peptide. CaM mutants containing a single or double cysteine residue around the EF hand and the target peptide-binding site of CaM were prepared according to established methods described under

EXPERIMENTAL PROCEDURES section. We prepared 10 CaM mutants, including A57C, N60C, D64C, M124C, E127C, A128C and M144C, in order to incorporate the photochromic PAM into the functional region of CaM. The crystal structures of the amino acid residues that were substituted by cysteine are shown in Fig. 1A. In order to ensure that the characteristics of the prepared CaM mutants were intact, we conducted urea–glycerol PAGE of the purified smooth muscle myosin after phosphorylation of the regulatory light chains (RLCs) to investigate the activation of smMLCK by the CaM mutants and determined that the CaM mutants retained the original function (Fig. 1B).

Modification of CaM Mutations with PAM—We employed PAM (Fig. 2), a sulfhydryl group-containing reactive photochromic compound, to incorporate the photochromic azobenzene moiety into the functional region of CaM. In order to determine the optimal conditions for specific labelling of the cysteine residues of CaM mutants, we conducted time-course studies and determined the reaction and concentration dependence of PAM for the CaM mutants. Previously, we had shown that PAM could successfully be incorporated into the specific cysteine residue of a kinesin mutant by increasing the concentration of PAM (*20*). The incorporation of PAM into the CaM mutant, N60C, was saturated in the reaction solution when the modification time was >1 min (Fig. 3A), and the amount of PAM was 2-fold higher than that of the CaM mutant (Fig. 3B). PAM was almost stoichiometrically incorporated into the CaM mutants (N60C : PAM = 1 : 1.07). PAM modified the other CaM mutants in a manner similar to its modification of N60C in the time-course and concentration-dependence reactions.

It has been demonstrated that the configurational state (*cis* or *trans*) of azobenzene and its derivatives can be monitored by UV/VIS light absorption spectroscopy (*10*, *14*). The UV/VIS light spectrum of PAM was similar to that of azobenzene (Fig. 4). The *trans* form of azobenzene exhibited maximum absorption at 315 nm in a solution of DMF, whereas that of its *cis* form was 330 nm under the same conditions. The irradiation of

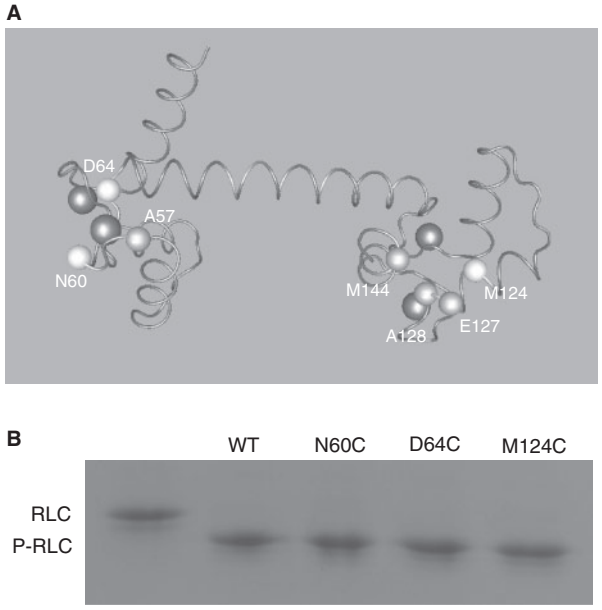

Fig. 1. **Location of the amino acids substituted by cysteine for the introduction of PAM in the crystal structure of the CaM.** (A) The α-carbons of the amino acids, A57, N60, D64, M124, E127, A128 and M144, substituted by cysteine are indicated in the space-filling model. The 3D structure was prepared using the molecular graphics program, Mol Feat, with the coordinate data (1CLL) of *Homo sapiens* CaM from the protein databank database. The amino acids, A57, N60, D64, M124, E127, A128 and M144, were modified with PAM. The α-carbons of the amino acids of the photocontrolled CaM mutants, N60C, D64C and M124C, are shown in white. The other α-carbons of the amino acids of the prepared CaM mutants are shown in grey. The calcium ion is shown in dark grey. (B) Urea–glycerol PAGE of smooth muscle myosin after phosphorylation of the RLC in the mixture containing 100 mM KCl, 30 mM Tris–HCl (pH 7.5), 8 mM $MgCl_2$, 0.1 mM $CaCl_2$, 6 mg/ml myosin, 15 μg/ml MLCK, 40 nM microcystin LR, 0.5 mM ATP and 5 μg/ml CaM. The positions of unphosphorylated and phosphorylated RLC (P-RLC) are shown. The first lane represents RLC before phosphorylation. The second, third, fourth and fifth lanes represent RLC after phosphorylation with CaM (WT), CaM (N60C), CaM(D64C) and CaM(M124C), respectively.

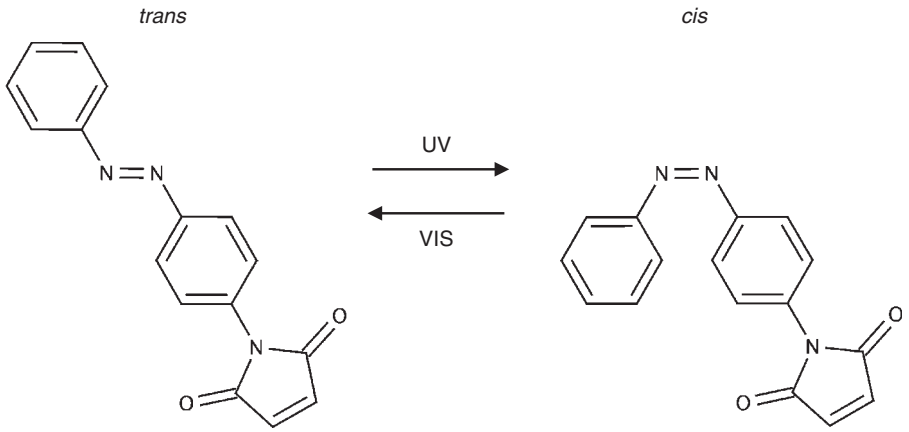

Fig. 2. **Schematic representation of photoisomerization of PAM.** The molecular structures of *cis* and *trans* PAM; UV light irradiation converts the *trans* form of PAM into the hydrophilic *cis* form. VIS light irradiation reverses the conversion.

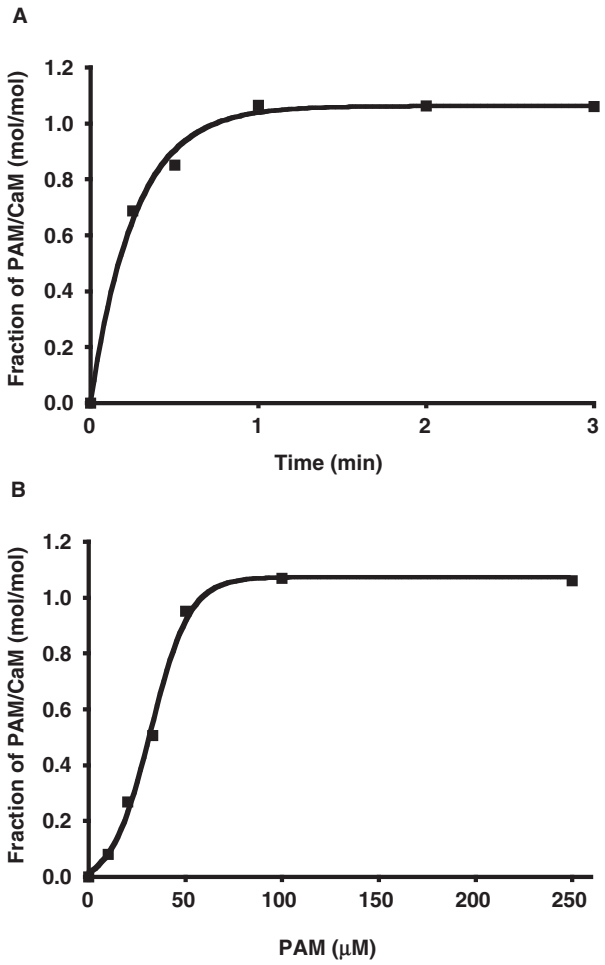

Fig. 3. **Time–course experiment and the concentration dependence of the incorporation of PAM into CaM (N60C).** (A) CaM of 50 μM was modified using a 2-fold molar excess of PAM at 25°C in a buffer containing 30 mM NaCl, 30 mM imidazole-HCl (pH 7) and 2% DMF for 0, 15, 30, 60, 120 and 180 s. The reaction was terminated by the addition of 5 mM DTT. The subsequent procedures were performed as described under EXPERIMENTAL PROCEDURES. (B) CaM of 50 μM (60°C) was reacted with PAM for 15 min at concentrations of 10, 20, 30, 50, 100 and 150 μM at 25°C in a buffer containing 30 mM NaCl, 30 mM imidazole-HCl (pH 7) and 2% DMF. The reaction was terminated by the addition of 5 mM DTT.

the *trans* form of PAM solution by UV light (366 nm) resulted in a significant reduction of the peak at 330 nm in the absorption spectrum. Following irradiation for 3 min, the alteration of the spectrum was saturated. In comparison with the spectral data previously reported (*24*), it was estimated that the solution contained ~75% *cis* and 25% *trans* forms of PAM. The spectral change in the UV/VIS absorbance of the CaM mutant, N60C, as modified by PAM (Fig. 4C and D) was similar to that of free PAM (Fig. 4A and B), indicating that PAM incorporated into N60C exhibited reversible isomerization between the *cis* and *trans* forms. The other mutants modified with PAM also showed reversible spectral changes upon UV/VIS light irradiation.

Interaction of CaM Mutants with the Target Peptide—M13-YFP, consisting of M13 peptide followed by YFP, was prepared in order to monitor the binding of CaM to the target M13 peptide. We investigated the interaction between CaM and M13-YFP by SEC–HPLC. Figure 5A shows the elution times for the standard proteins used on the SEC column. The elution time of M13-YFP and CaM are 9.5 and 8.5 min, respectively. The elution time of CaM corresponded to an apparent molecular weight of 43 kDa, instead of the real molecular weight of 17 kDa. This phenomenon may be due to the unique dumbbell shape of CaM and is supported by a previous report of metallothionein, a dumbbell-shape protein like CaM, in which this phenomenon is explained based on its Stokes' radius (*25*). Another possible explanation for this phenomenon is the formation of CaM dimer. Previously, it has been reported that CaM forms a dimer only under appropriate condition (*26*). Figure 5C shows elution pattern for the mixture of the CaM (WT) and M13-YFP at a high Ca^{2+} concentration (pCa 6.5) by SEC–HPLC. The elution time of the M13-YFP and CaM complex is 8 min, which is consistent with the time estimated from the standard elution time. Figure 5B shows SDS–PAGE analysis of elution pattern of Fig. 5C, which shows the elution fraction at every 10 s. The result of the M13-YFP eluted with CaM (Fig. 5B, lanes 2–5) indicates that the peak at 8 min is the M13-YFP and CaM complex. The area of the peak corresponding to the complex of M13-YFP and CaM decreased and the area of the peak corresponding to the free M13-YFP increased broadly, with reducing Ca^{2+} concentration (Fig. 5C–F). Under low Ca^{2+} concentration (pCa > 7.5), the complex of CaM(WT) and M13-YFP (Fig. 5F) was not observed at all. The insets in Fig. 5C–F show the protein staining bands of M13-YFP on SDS–PAGE that are consistent with elution pattern by SEC–HPLC. The sample of the M13-YFP that we have prepared in this study has been partially degraded to the slightly smaller molecule. As shown in Fig. 5F inset lane 9–10, doublet bands corresponding to the intact M13-YFP and degraded M13-YFP were observed. We have analysed the structure of the degraded M13-YFP using time-of-flight mass spectrometry and protein sequencer. It has been shown that the degraded M13-YFP lacks the N-terminal six amino acids (MRWKKN) in the M13 region. Previously it has been demonstrated that the N-terminal six amino acids are essential to bind to CaM (*31*).

In Fig. 5C–F, the peak corresponding to free M13-YFP is broadly distributed due to overlapping of degraded M13-YFP and intact M13-YFP. Fluorescence intensity of the region at 9.5 min in the peak did not depend on Ca^{2+} concentration, because of the existence of the degraded M13-YFP. SDS–PAGE analysis of the fractions on the HPLC clearly demonstrated that the degraded M13-YFP eluted at 9.5 min. On the other hand, the intact M13-YFP bound to CaM eluted at 8 min. And the free intact M13-YFP eluted broadly at 9.5–12 min (Fig. 5C).

Figure 6A shows the alterations in the interaction between M13-YFP and various CaM mutants under various Ca^{2+} concentrations. The association between CaMs and M13-YFP increased with increasing Ca^{2+}

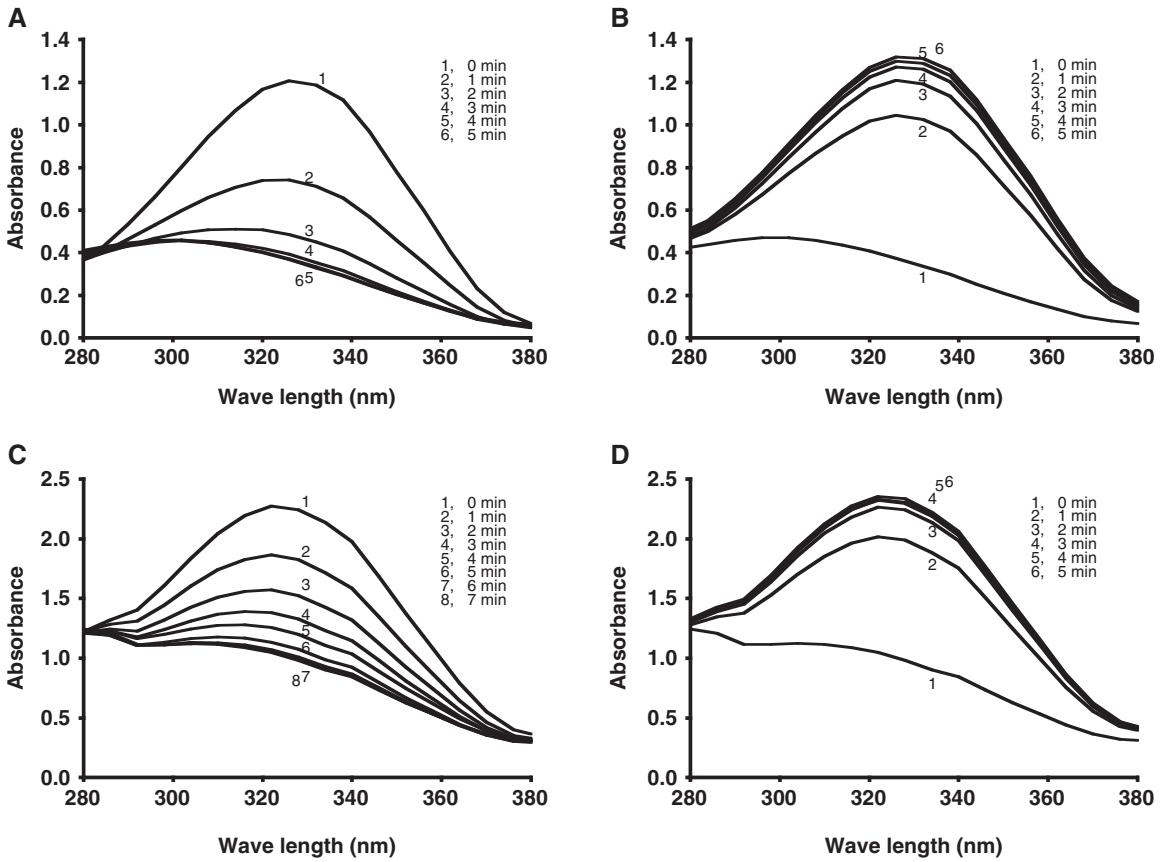

Fig. 4. **Changes in the absorption spectra of free PAM and the PAM–CaM (N60C) mutant induced by UV and VIS light irradiation.** (A) Free PAM of 50 μM in a solution of 70% ethanol and 2% DMF was irradiated by UV light at 366 nm for 1–5 min at room temperature. (B) Free PAM of 50 μM irradiated by UV light at 366 nm for 5 min was subsequently irradiated by fluorescent room light for 1–5 min at room temperature. (C) PAM–CaM (N60C) of 50 μM mutant in a solution of 30 mM NaCl, 30 mM Tris–HCl (pH 7.5), 1 mM DTT and 2% DMF was irradiated by UV light at 366 nm for 1–7 min at room temperature. (D) PAM–CaM (50 μM) (N60C) mutant irradiated by UV light at 366 nm for 7 min was subsequently irradiated by fluorescent room light for 1–5 min at room temperature.

concentrations and saturation was observed at pCa < 6. The interactions of N60C, D64C, M124C and WT of CaM with M13-YFP varied significantly over a range of pCa from 5.75 to 6.75, pCa from 6 to 7, pCa from 6.25 to 7.25 and pCa from 6.25 to 7.5, respectively. Ca^{2+} concentration-dependent binding of M13 to N60C, D64C and M124C slightly shifted to higher Ca^{2+} concentrations as compared with the binding of WT CaM. However, at high concentrations of Ca^{2+}, the affinities of the CaM mutants for M13-YFP were almost identical to that of the WT (Fig. 6B).

Photocontrol of PAM–CaM Binding to the Target Peptide—Figure 7 shows the alterations in the interaction between M13-YFP and the CaM mutants modified by PAM accompanied by *cis–trans* isomerization of PAM under various Ca^{2+} concentrations. The ratio of M13-YFP bound to PAM–CaM (N60C)-VIS or (N60C)-UV increased according to the Ca^{2+} concentration (Fig. 7A). The binding of M13-YFP to PAM-CaM (N60C)-VIS or (N60C)-UV reached saturation at pCa 5, and the maximum ratios of M13-YFP bound to N60C-PAM-VIS and N60C-PAM-UV were ~0.5 and 0.94 mol/mol, respectively. Figure 8A shows the alterations in the binding of M13-YFP to PAM-CaM (N60C) induced by UV/VIS light irradiation at pCa 6. The binding of M13-YFP to PAM-CaM (N60C) increased ~5-fold (0.12–0.64 mol/mol) after the first exposure to UV light irradiation and subsequently decreased to 0.17 mol/mol, because it was restored by VIS light irradiation. Further, the second exposure to UV light irradiation increased the binding to 0.62 mol/mol, which was almost the same level as that after the first exposure to UV irradiation. The alterations in the interaction induced by alternate UV–VIS light irradiation were apparently reversible. Even after alternating the UV/VIS light irradiation twice, the binding ability of PAM-CaM (N60C) to M13-YFP was retained. These reversible alterations were observed at pCa < 6.25 (Fig. 7A). Alterations in the binding of M13-YFP to PAM-CaM (D64C) and PAM-CaM (N60C) brought about by exposure to UV/VIS light irradiation were similar (Figs 7B and 8B).

Interestingly, interaction of PAM-M124C with M13-YFP was decreased by UV light irradiation and increased by VIS light irradiation (Figs 7C and 8C), contrary to its interaction with the mutants, D64C and N60C. The reversible alterations were observed in a range from

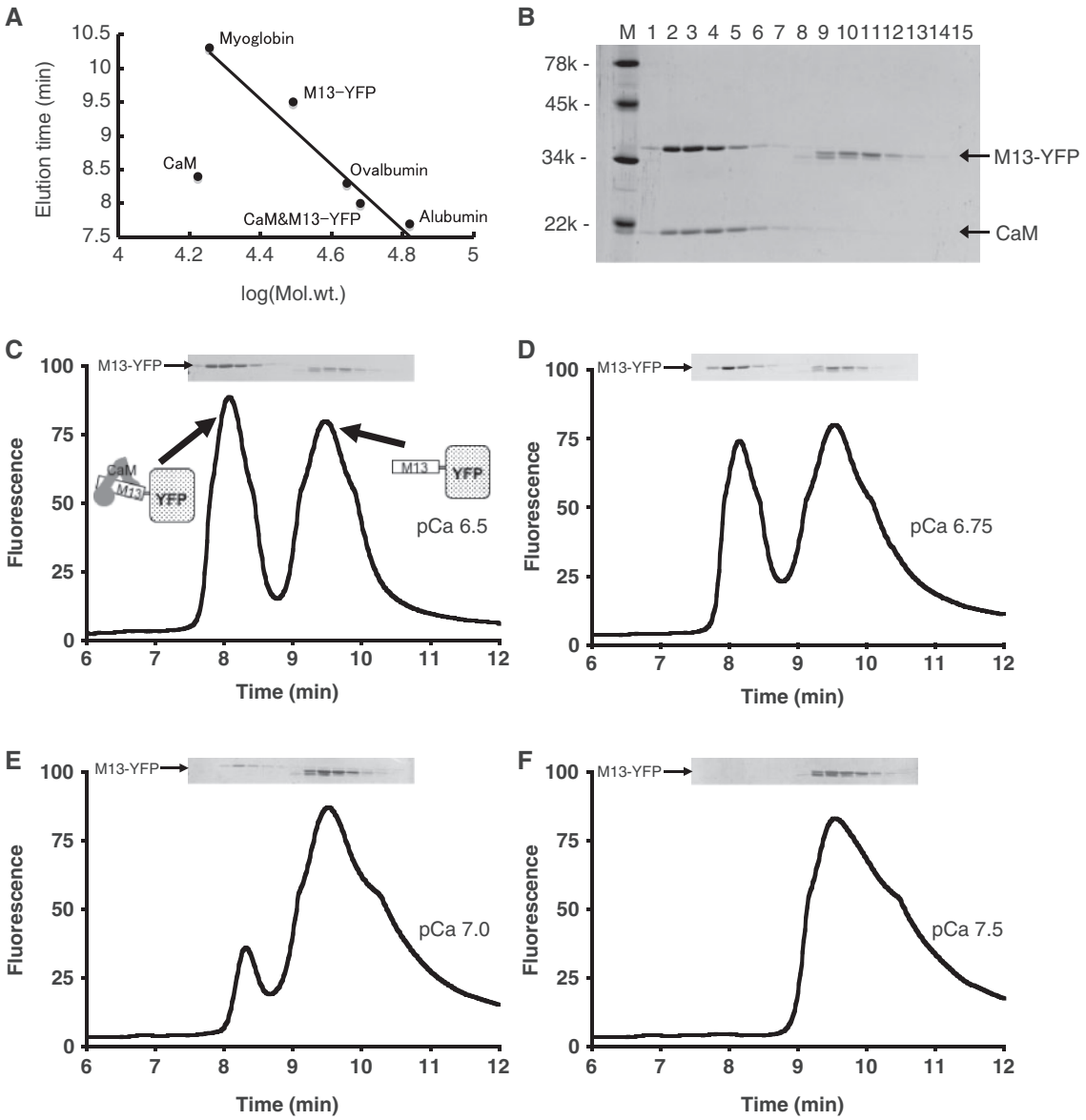

Fig. 5. **Monitoring the interaction of CaM and M13-YFP and its dependence on Ca^{2+} concentration by SEC–HPLC.** (A) The elution times for CaM, M13-YFP, the CaM-M13-YFP complex and the standard proteins (albumin, ovalbumin and myoglobin) used for calibration of the SEC–HPLC (TSKgel G3000SW column; Ca-EGTA buffer). (B) The SDS–PAGE of eluted fraction of a mixture of 10 μM CaM (WT) and 20 μM M13-YFP in a Ca-EGTA buffer prepared with pCa 6.5 by SEC–HPLC corresponds to the result of SDS–PAGE in inset of Fig. 5C. M, molecular weight markers; lanes 1–15 represent eluted fractions at every 10 s from 7 min 50 s to 9 min 20 s. (C–F) A mixture of 10 μM CaM (WT) and 20 μM M13-YFP in a Ca-EGTA buffer prepared with pCa 6.5 (C), pCa 6.75 (D), pCa 7.0 (E) and pCa 7.5 (F) was monitored by SEC–HPLC with an excitation wavelength of 475 nm and fluorescence monitoring at 527 nm. The first fluorescence peak detected at ~8 min indicated the complex of CaM and M13-YFP. The second fluorescence peak detected at ~9.5 min indicated M13-YFP (inset); SDS–PAGE analysis of the eluted fraction at every 10 s is showed M13-YFP bands.

pCa 5.5 to 7 (Fig. 7C), indicating that M124C-PAM has a higher affinity for the Ca^{2+} ion than PAM–CaM (N60C or D64C). The binding of M13-YFP to PAM-CaM (M124C)-VIS or (M124C)-UV reached saturation at pCa 5.5. At this Ca^{2+} concentration, the maximum ratios of M13-YFP bound to PAM–CaM (M124C) under both UV and VIS light irradiation were ~1.0 mole/mole. From these experimental results, it is clear that PAM–CaM binding to the target peptide is reversibly controlled by UV/VIS light irradiation. We also investigated other CaM mutants, namely A57C, E127C, A128C, M144C, R74C and E83C. However, these mutants did not show any reversible alterations in binding to M13-YFP accompanied by *cis–trans* isomerization when modified by PAM.

DISCUSSION

The aim of this study was to photocontrol the regulatory proteins as bionanomachines using photochromic molecules. CaM is a Ca^{2+}-binding protein and is one of the

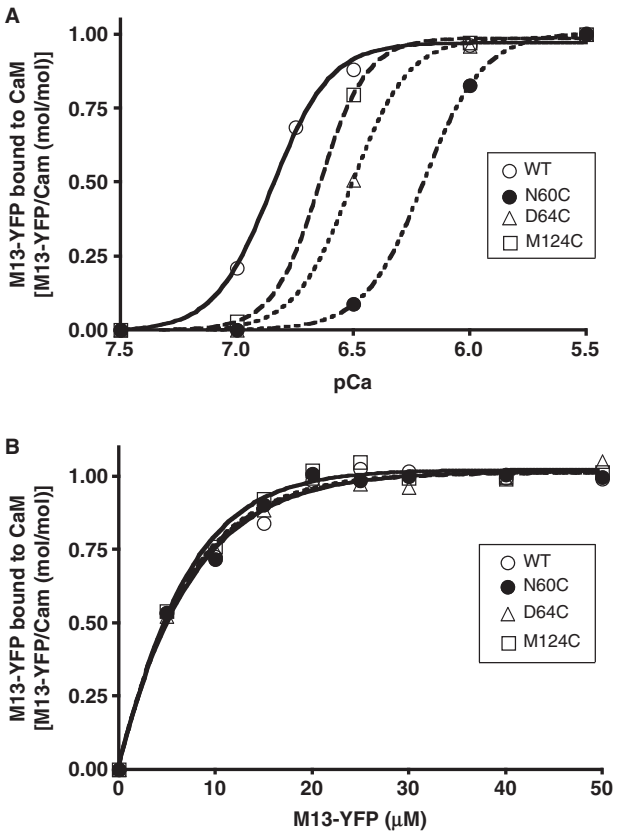

Fig. 6. **Comparison of the various CaMs binding to M13-YFP and their dependence on Ca^{2+} and M13-YFP concentrations.** (A) A mixture of 10 μM of the various CaM mutants and 20 μM of M13-YFP in a Ca-EGTA buffer (pCa 5.5–7.5) was monitored by fluorescence SEC–HPLC. CaM WT and the CaM mutants, N60C, D64C and M124C, are represented by the open circle, closed circle, triangle and square, respectively. The excitation and emission wavelengths were 475 and 527 nm, respectively. (B) A mixture of 10 μM of the various CaM mutants and 0–50 μM of M13-YFP in a Ca-EGTA buffer (pCa 5.0) was monitored by SEC–HPLC. CaM WT and the CaM mutants, N60C, D64C and M124C, are represented by the open circle, closed circle, triangle and square, respectively. The excitation and emission wavelengths were 475 and 527 nm, respectively.

key regulatory proteins in cell signal transduction. Numerous enzymes involved in cell function are regulated by CaM. Therefore, photocontrol of CaM function will lead to regulation of its target enzymes activities and may help studies on cell function. Moreover, CaM has superior stability of structure and function. Denatured CaM is readily renatured on removal of the factors that induce denaturation. Therefore, the technique of controlling functional biomaterials using photochromic molecules may also be applicable to the field of nanotechnology.

In this study, we demonstrated that binding of CaM modified with a photochromic compound to the target peptide can be reversibly regulated by UV–VIS light irradiation. The most important aspect of regulation of CaM function is designing the site to be modified by the photochromic molecules. The direct incorporation of photochromic molecules into the significant interfaces between CaM and its ligands may completely abolish the interaction due to its stearic hindrance. Such direct incorporation into the interfaces may be effective for caging reagents whose bulky groups are eliminated from the modification site by exposure to UV irradiation. On the other hand, photochromic molecules change their structures and properties, but remain intact at the modified sites. Therefore, photochromic molecules should be incorporated into sites that are slightly away from the significant key regions. Further, the two isomers induced by UV and VIS light irradiation must affect the key regions differently from each other.

We designed two types of CaM mutants with a single cysteine residue in the functional region in order to specifically incorporate the azobenzene derivative. The first type of the CaM mutant had a single cysteine in the N-terminal EF motif. Ca^{2+} binding to CaM triggered the opening of the angle between the two helices resulting in the so-called 'open' conformation (*27–29*). The central linker of the open conformation retained the α-helix in the absence of a target peptide. When the CaM bound to the target peptide, the central helix of the CaM partially melted and got entwined around the hydrophobic α-helix of the target peptide (*30*). Therefore, the EF motif

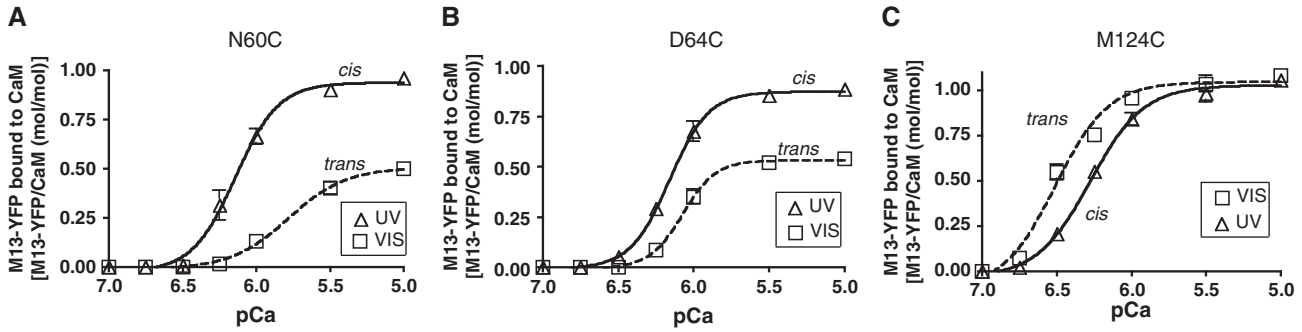

Fig. 7. **The effect of UV–VIS light irradiation on the ratios of the various PAM–CaM mutants bound to M13-YFP and their dependence on Ca^{2+} concentration.** The CaM mutants (A) N60C, (B) D64C and (C) M124C were irradiated by UV and VIS light alternately under the same conditions described in the legend for Fig. 6. A mixture of 10 μM of various irradiated PAM–CaM mutants and 20 μM of M13-YFP in a Ca-EGTA buffer with pCa ranging from 5 to 7 was monitored by SEC–HPLC. In a Ca-EGTA buffer with pCa ranging from 5 to 7, the ratios of the various PAM–CaM mutants bound to M13-YFP varied alternately between UV and VIS light irradiation. UV and VIS light irradiation are indicated by the triangle and square, respectively. The error bars indicate SD.

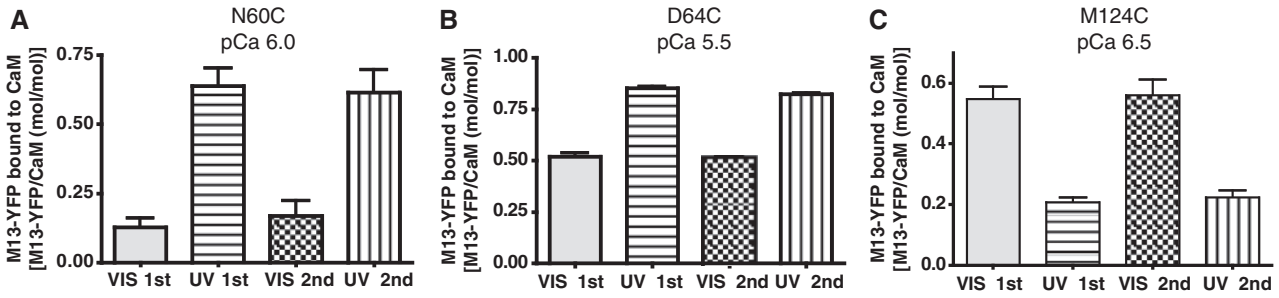

Fig. 8. **Reproducible reversibility of the photocontrol ratios of the various PAM–CaM mutants bound to M13-YFP.** For *cis* state conversion, the PAM–CaM mutants were irradiated by UV light at 366 nm for 7 min on ice; for the *trans* state conversion, the PAM–CaM mutants were irradiated by fluorescent room light for 3 min on ice. The mixture of 10 μM of various irradiated PAM–CaM mutants and 20 μM of M13-YFP in Ca-EGTA buffer with varying Ca^{2+} concentrations was monitored by SEC–HPLC. The alternating UV–VIS light irradiation was repeated twice. The ratios of the various PAM–CaM mutants in the Ca-EGTA buffer with varying Ca^{2+} concentrations, *i.e.* (A) N60C at pCa 6.0, (B) D64C at pCa 5.5 and (C) M124C at pCa 6.5, bound to M13-YFP vary alternately between UV and VIS light irradiation. The error bars indicate SD.

to which the initial signal of Ca^{2+} was bound comprised the key region to regulate CaM function. CaM has two EF hands (EF1 and EF2) in its N-terminal domain and two EF hands (EF3 and EF4) in its C-terminal half. The affinities of EF3 and EF4 for Ca^{2+} are extremely strong and higher than those of EF1 and EF2. It is known that Ca^{2+}-dependent regulation of physiological CaM function is based on EF1 and EF2. Ca^{2+} interacts with the oxygen atom in the six residues of the EF hand. The first three and last three ligands in the geometry of the six ligands for Ca^{2+} are defined as *X*, *Y* and *Z*-axes and $-Y$, $-X$ and $-Z$-axes, respectively (*6*). We prepared the mutants, A57C, N60C and D64C, each of which had a single cysteine positioned around the EF hand. As expected, the mutants N60C and D64C modified by PAM showed photoregulation on binding to the target peptide. However, PAM-A57C was not photocontrolled. The residues of N60 and D64 are in EF2 in the N-terminal domain and function as Z and −X ligands. On the other hand, the A57 residue is not a ligand for Ca^{2+}, and the side chain of the A57 residue protrudes into the surface of the crystal structure. Therefore, modification of the A57 residue with PAM does not affect its affinity for Ca^{2+}.

Azobenzene is a photochromic molecule and changes its shape significantly and reversibly on light irradiation. It assumes the compact structure of the *cis* isomer upon UV light irradiation and the elongated structure of the *trans* isomer upon VIS light irradiation. As shown in Fig. 7, Ca^{2+} concentration-dependent binding of N60C and D64C modified with *cis*-PAM to M13 shifted to lower Ca^{2+} concentrations as compared with the binding of N60C and D64C modified with *trans*-PAM.

As the binding activity of N60C modified with *cis*-PAM and that of intact N60C were almost identical, the EF hand structure in unmodified N60C may have been retained in *cis*-PAM-N60C. The lone-pair electrons of the azo group of the *cis* form of PAM may be interacting with Ca^{2+}. On the other hand, the elongated *trans* isomer may change the conformation of the EF hand, thereby resulting in reducing its affinity to Ca^{2+}.

Previously, we had successfully regulated conformational changes in skeletal muscle myosin by photoisomerization of azobenzene derivatives. The bifunctional azobenzene derivative, ABDM, was incorporated into the SH1–SH2 region of skeletal muscle myosin S1, which is a potential energy-transducing site. It was demonstrated that *cis–trans* isomerization of ABDM reversibly promotes a swing in the lever arm of S1 in a direction opposite to that of the swing induced by ATP binding (*10*). However, it is difficult to analyse the localized conformational change in detail at the region modified by the azobenzene derivative owing to its high molecular mass. On the other hand, the structure of CaM at the amino acid level has been well studied by NMR owing to its smaller molecular mass. Therefore, it is expected that the molecular mechanism of photoregulation by azobenzene derivatives will be clarified in the near future.

The second type of CaM mutants has a single cysteine residue in the hydrophobic anchoring region that interacts with the target peptide. In this study, we employed M13 peptide as the target peptide. The first major hydrophobic anchor (Trp) of the M13 peptide is thought to be important for the interaction with CaM (*8*). The L105, M124, E127, A128 and M144C residues in the C-terminal region of CaM are the candidates that interact with the Trp residue in M13. The Trp residue is embedded in a large hydrophobic pocket of CaM consisting of Phe 89, Phe 92, Ile 100, Met 109, Val 121, Met 124, Ile 125, Val 136, Phe141 and Met 145 (*31*). Azobenzene derivatives of photochromic compounds such as PAM are known to have a hydrophilic *cis* isomer and a hydrophobic *trans* isomer (*32*). The hydrophobic interaction between the amino acid residues of CaM and the target peptide is expected to be reduced by isomerization to the hydrophilic *cis*-azobenzene on the hydrophobic interaction site. We prepared CaM mutants, M124C, E127C, A128C and M144C. Binding of PAM–CaM (M124C) to the target peptide was successfully photocontrolled, but that of PAM–CaM (E127C), PAM–CaM (A128C) and PAM–CaM (M144C) to the target peptide could not be photocontrolled. As shown in Fig. 7C, Ca^{2+} concentration-dependent binding of *trans*-PAM–CaM (M124C) to the M13 peptide shifted to lower Ca^{2+} concentrations as compared with that of *cis*-PAM–CaM (M124C). The *trans*

form of PAM may stearically interrupt the interaction of CaM with the M13 peptide because the *trans* form of PAM is bulkier than its *cis* form. However, in fact, *trans*-PAM-M124C showed higher binding to M13 than *cis*-PAM-M124C. The possible explanation is that the hydrophobicity of the *trans* form of PAM in M124C may have slightly increased the affinity of CaM to the M13 peptide.

We have previously demonstrated a similar method of photoregulation of kinesin on the basis of the alteration of its hydrophobicity accompanied by *cis–trans* isomerization of PAM (*20*). We prepared five kinesin motor domain mutants—A247C, L249C, A252C, G272C and S275C—containing a single reactive cysteine residue in loops, L11 and L12. These loops are considered to be the key regions for the functioning of kinesin as a motor protein. PAM was stoichiometrically incorporated into the cysteine residues in the loops of the mutants. Upon irradiation with UV and VIS light, the PAM-modified S275C mutant exhibited reversible alterations in its ATPase activity accompanied by *cis–trans* isomerization. We proposed a possible explanation that the hydrophobic *trans* PAM incorporated in the middle of L12 interacts with the hydrophobic cluster in α4, thereby resulting in significant conformational changes in L12.

From this experimental result, we propose some control models based on the isomerization of photochromic compounds. New CaM mutants should be prepared for further efficient regulation based on these control models. In this study, it was demonstrated that modification of the residues in EF2 and EF4P with PAM were effective for photocontrol. The same positions (Z or X) of the other EF hand may also be effective and are used because nearly four EF hand sequences of CaM are conserved. Incorporation of more than one PAM into some EF hands may also introduce significant photocontrol.

In conclusion, we successfully photocontrolled CaM function using an azobenzene derivative of a photochromic compound. Since CaM regulates a multitude of functional proteins, photocontrollable CaM could be applied to the photoregulation of the CaM target enzymes.

FUNDING

Grant-in-Aid for Scientific Research in Innovative Areas from the Ministry of Education, Culture, Sports, Science and Technology (MEXT); Sasagawa Scientific Research Grant from the Japan Science Society.

CONFLICT OF INTEREST

None declared.

REFERENCES

1. Chin, D. and Means, A.R. (2000) Calmodulin: a prototypical calcium sensor. *Trends Cell Biol.* **10**, 322–328
2. Persechini, A. and Stemmer, P.M. (2002) Calmodulin is a limiting factor in the cell. *Trends Cardiovasc. Med.* **12**, 32–37
3. Kamm, K.E. and Stull, J.T. (2001) Dedicated myosin light chain kinases with diverse cellular functions. *J. Biol. Chem.* **276**, 4527–4530
4. Kawasaki, H. and Kretsinger, R.H. (1994) Calcium-binding proteins. 1: EF-hands. *Protein Profile* **1**, 343–517
5. Kawasaki, H. and Kretsinger, R.H. (1995) Calcium-binding proteins 1: EF-hands. *Protein Profile* **2**, 297–490
6. Grabarek, Z. (2006) Structural basis for diversity of the EF-hand calcium-binding proteins. *J. Mol. Biol.* **359**, 509–525
7. Chou, J.J., Li, S., Klee, C.B., and Bax, A. (2001) Solution structure of Ca(2+)-calmodulin reveals flexible hand-like properties of its domains. *Nature Struct. Biol.* **8**, 990–997
8. Meador, W.E., Means, A.R., and Quiocho, F.A. (1992) Target enzyme recognition by calmodulin: 2.4 A structure of a calmodulin-peptide complex. *Science* **257**, 1251–1255
9. Meador, W.E., Means, A.R., and Quiocho, F.A. (1993) Modulation of calmodulin plasticity in molecular recognition on the basis of x-ray structures. *Science* **262**, 1718–1721
10. Rau, H. (1990) Azo Compounds, in Photochromism in *Molecules and Systems* (Durr, H. and Bouas-Laurent, H., eds), pp. 165–192, Elsevier, Amsterdam
11. Ichimura, K., Seki, T., Kawanishi, Y., Suzuki, Y., Sakuragi, M., and Tamaki, T. (1996) Photocontrol of liquid crystal alignment by "command surface" in *Photoreactive Materials for Ultrahigh Density Optical Memory* (Irie, M., ed.), pp. 55–88, Elsevier, Amsterdam
12. Irie, M., Fukaminato, T., Sasaki, T., Tamai, N., and Kawai, T. (2002) Organic chemistry: a digital fluorescent molecular photoswitch. *Nature* **420**, 759–760
13. Kimura, K., Mizutani, R., Suzuki, T., and Yokoyama, M. (1998) Photochemical ionic-conductivity switching systems of photochromic crown ethers for information technology. *J. Inclus. Phenom. Mol. Recognit. Chem.* **32**, 295–310
14. Rau, H. (1990) Photoisomerization of azobenzenes in *Photochemistry and Photophysics* (Rabek, J.F., ed.) Vol. II, pp. 119–141, CRC, Boca Raton, FL
15. Kumita, J.R., Smart, O.S., and Woolley, G.A. (2000) Photocontrol of helix content in a short peptide. *Proc. Natl Acad. Sci. USA* **97**, 3803–3808
16. Flint, D.G., Kumita, J.R., Smart, O.S., and Woolley, G.A. (2002) Using an azobenzene cross-linker to either increase or decrease peptide helix content upon trans-to-cis photoisomerization. *Chem. Biol.* **9**, 391–397
17. Willner, I., Rubin, S., and Riklin, A. (1990) Photoregulation of papain activity through anchoring photochromic azo groups to the enzyme backbone. *J. Am. Chem. Soc.* **113**, 3321–3325
18. Willner, I., Rubin, S., and Riklin, A. (1996) Control of the structure and functions of biomaterials by light. *Angew. Chem. Int. Ed. Engl.* **35**, 367–385
19. Umeki, N., Yoshizawa, T., Sugimoto, Y., Mitsui, T., Wakabayashi, K., and Maruta, S. (2004) Incorporation of an azobenzene derivative into the energy transducing site of skeletal muscle myosin results in photo-induced conformational changes. *J. Biochem.* **136**, 839–846
20. Yamada, M.D., Nakajima, Y., Maeda, H., and Maruta, S. (2007) Photocontrol of kinesin ATPase activity using an azobenzene derivative. *J. Biochem.* **142**, 691–698
21. Persechini, A., Blumenthal, D.K., Jarrett, H.W., Klee, C.B., Hardy, D.O., and Kretsinger, R.H. (1989) The effects of deletions in the central helix of calmodulin on enzyme activation and peptide binding. *J. Biol. Chem.* **264**, 8052–8058
22. Ruppel, K.M., Uyeda, T.Q.P., and Spudich, J.A. (1994) Role of highly conserved lysine 130 of myosin motor domain. In vivo and in vitro characterization of site specifically mutated myosin. *J. Biol. Chem.* **269**, 18773–18780
23. Tsien, R. and Pozzan, T. (1989) Measurement of cytosolic free Ca2+ with quin2. *Methods Enzymol.* **172**, 230–262
24. Behrendt, R., Renner, C., Schenk, M., Wang, F., Wachtveitl, J., Oesterhelt, D., and Moroder, L. (1999) Photomodulation of the conformation of cyclic peptides

with azobenzene moieties in the peptide backbone. *Angew. Chem. Int. Ed. Engl.* **38**, 2771–2774
25. Nordberg, G.F., Nordberg, M., Piscator, M., and Vesterberg, O. (1972) Separation of two forms of rabbit metallothionein by isoelectric focusing. *Biochem. J.* **126**, 491–498
26. Lafitte, D., Heck, A.J., Hill, T.J., Jumel, K., Heading, S.E., and Derrick, P.J. (1999) Evidence of noncovalent dimerization of calmodulin. *Eur. J. Biochem.* **261**, 337–344
27. Zhang, M., Tanaka, T., and Ikura, M. (1995) Calcium-induced conformational transition revealed by the solution structure of apo calmodulin. *Nat. Struct. Biol.* **2**, 758–767
28. Kuboniwa, H., Tjandra, N., Grzesiek, S., Ren, H., Klee, C.B., and Bax, A. (1995) Solution structure of calcium-free calmodulin. *Nat. Struct. Biol.* **2**, 768–776
29. Finn, B.E., Evenas, J., Drakenberg, T., Waltho, J.P., Thulin, E., and Forsen, S. (1995) Calcium-induced structural changes and domain autonomy in calmodulin. *Nat. Struct. Biol.* **2**, 777–783
30. Tanaka, T., Ohmura, T., and Hidaka, H. (1982) Hydrophobic interaction of the Ca2+-calmodulin complex with calmodulin antagonists. Naphthalenesulfonamide derivatives. *Mol. Pharmacol.* **22**, 403–407
31. Hultschig, C., Hecht, H.J., and Frank, R. (2004) Systematic delineation of a calmodulin peptide interaction. *J. Mol. Biol.* **343**, 559–568
32. Seki, T., Sekizawa, H., Morino, S., and Ichimura, K. (1998) Inherent and cooperative photomechanical motions in monolayers of an azobenzen containing polymer at the air–water interface. *J. Phys. Chem.* **102**, 5313–5321